Radiation Dose Estimates in Humans for ^{11}C-Acetate Whole-Body PET

Marc A. Seltzer, MD[1]; Shamim A. Jahan, MPH[1]; Richard Sparks, PhD[2]; David B. Stout, PhD[1]; Nagichettiar Satyamurthy, PhD[1]; Magnus Dahlbom, PhD[1]; Michael E. Phelps, PhD[1]; and Jorge R. Barrio, PhD[1]

[1]Department of Molecular and Medical Pharmacology, Ahmanson Biological Imaging Center, University of California at Los Angeles School of Medicine, Los Angeles, California; and [2]CDE Dosimetry Services, Knoxville, Tennessee

^{11}C-Acetate is currently being investigated as a new tracer for imaging neoplasms, most notably prostate cancer and its metastases. Previously reported dose estimates for ^{11}C-acetate prepared by the Oak Ridge Institute for Science and Education (ORISE) were based on a simple 3-compartment model in which all activity not measured in blood or excretion via breath was assumed to reside in the heart. Because all organs are involved in acetate metabolism to some extent, these estimates might overestimate heart and underestimate other organ dosimetry. Dynamic whole-body ^{11}C-acetate PET was therefore performed on 6 healthy human volunteers. Measured dose estimates for all target organs were compared with the existing ORISE values. **Methods:** After transmission scanning had been performed for measured attenuation, 525 MBq of ^{11}C-acetate were injected intravenously, and 5 sequential whole-body emission scans were obtained from the head to mid thighs. Regions of interest were drawn to encompass the entire activity in all visible organs at each time point. Time–activity data were fit in a least-squares sense to obtain residence times. Absorbed dose estimates were determined using MIRDOSE3.1 software. **Results:** The effective dose was 0.0049 mSv/MBq. The organs receiving the highest absorbed doses were the pancreas (0.017 mGy/MBq), bowel (0.011 mGy/MBq), kidneys (0.0092 mGy/MBq), and spleen (0.0092 mGy/MBq). No urinary excretion of tracer was measurable. **Conclusion:** Using these new estimates for ^{11}C-acetate dosimetry, the maximum injected activity under Radioactive Drug Research Committee limits can be raised up to 5-fold over the limit imposed by the previous ORISE estimates. A higher injected activity would improve counting statistics and, it is hoped, overall image quality and tumor detection with whole-body ^{11}C-acetate PET.

Key Words: ^{11}C-acetate; dosimetry; PET

J Nucl Med 2004; 45:1233–1236

For a variety of cancer types, 1-^{11}C-acetate (^{11}C-acetate) is being investigated as a tumor imaging agent. In prostate cancer, ^{11}C-acetate PET studies have been performed that demonstrate a high concentration of tracer in primary and metastatic lesions (*1–3*). Acetate accumulation in tumor cells appears to be due to the low oxygen consumption and enhanced lipid synthesis of these cells. Preliminary studies indicate that certain prostate tumors prefer ^{11}C-acetate to ^{18}F-FDG as a substrate for cellular metabolism. Figure 1 shows an example of a patient with advanced prostate cancer and metastatic lesions that were better visualized with ^{11}C-acetate than with ^{18}F-FDG whole-body PET. An additional potential advantage of ^{11}C-acetate over ^{18}F-FDG is that ^{11}C-acetate is not excreted by the kidneys and therefore results in no measurable tracer activity in the urinary bladder (*3*). In the evaluation of pelvic malignancies such as prostate cancer, the absence of urinary tracer excretion may allow improved detection of pelvic lymph node metastases and local pelvic tumor recurrence.

The only reported internal dosimetry data for ^{11}C-acetate are the Oak Ridge Institute for Science and Education (ORISE) dose estimates (*4*), which were based on experiments performed on dogs (*5*). The results of these experiments were used by ORISE to create a simple 3-compartment model in which all activity not measured in blood or excretion via breath was assumed to reside in the heart. Because all organs are involved in acetate metabolism, the ORISE estimates would likely overestimate heart and underestimate other organ dose estimates. Although the ORISE estimates were correctly and appropriately performed given the limited data at the time, more accurate dosimetry estimates could be obtained using a more complete set of data. Thus, whole-body ^{11}C-acetate PET was performed on 6 healthy human volunteers, and the resulting dose estimates were compared with the ORISE estimates.

MATERIALS AND METHODS

Subjects

Six healthy men (mean age ± SD, 66 ± 11 y; age range, 54–78 y) with no clinical evidence of prostate cancer were enrolled. All men had a normal serum prostate-specific antigen level (less than 3.0 ng/mL) and normal findings on digital rectal examination. The study was approved by the Medical Institutional Review Board, and informed written consent was obtained from each study participant.

Received Sep. 17, 2003; revision accepted Jan. 21, 2004.

For correspondence or reprints contact: Marc A. Seltzer, MD, Department of Radiology, Dartmouth-Hitchcock Medical Center, One Medical Center Dr., Lebanon, NH 03756.

E-mail: Mseltzer@hitchcock.org

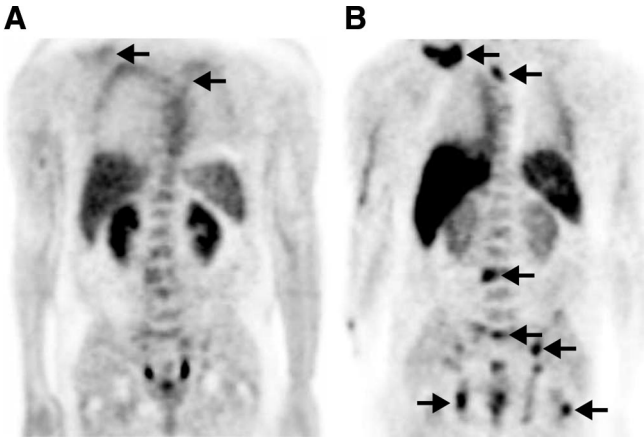

FIGURE 1. Coronal whole-body PET images obtained with ^{18}F-FDG (A) and ^{11}C-acetate (B) for a patient with advanced prostate cancer. Multiple osseous metastases (arrows) were better visualized with ^{11}C-acetate PET than with ^{18}F-FDG PET. Pelvic activity seen in A represents urine in the distal ureters and bladder.

Whole-Body PET Protocol

PET was performed using 1 of 2 high-resolution dedicated systems (ECAT EXACT or ECAT HR+; CTI/Siemens Medical Systems, Inc.). The characteristics of these scanners have been described previously (*6,7*). Iterative image reconstruction with measured segmented attenuation-correction was performed for all studies (*8,9*). The resolution for reconstructed images ranged from 8 to 12 mm. Image data were converted from counts/s/pixel to MBq/mL using a calibration constant derived from imaging a known activity concentration of ^{18}F in a cylindric phantom.

The tracer ^{11}C-acetate was produced from carbon dioxide using a method described previously (*10*). All volunteers fasted for at least 6 h before radioisotope injection. After a whole-body transmission scan had been obtained (used to perform attenuation correction of the emission data), an average dose of 525 MBq of ^{11}C-acetate was injected intravenously. Five sequential whole-body emission scans (6 bed positions per scan) were acquired from the head to the mid thighs at approximately 2, 14, 28, 52, and 76 min after injection. The duration of the first 2 whole-body scans was 12 min each (2 min per bed position), and for the subsequent 3 whole-body scans the duration was 24 min each (4 min per bed position).

The major organs considered as measured source organs were the heart, kidneys, lungs, liver, spleen, pancreas, salivary glands, lumbar spine, stomach, and bowel. An example of whole-body PET images at 2 representative time points is shown in Figure 2. At the early time point, intense tracer uptake is seen in the salivary glands, heart, pancreas, kidneys, spleen, and bowel. At the late time point, activity has almost completely cleared from the heart and kidneys (reflecting the rapid oxidative metabolism of these organs). Activity is significantly retained within the salivary glands, pancreas, liver, spleen, and bowel.

Organ Time–Activity Measurements

Reconstructed coronal PET images with a slice thickness of 5.1 mm were used to identify and measure the activity of each source organ listed in Table 1. Organ regions of interest (ROI) were manually drawn across all image planes at each time point to account for the entire activity within each organ over time. With the exception of the lungs, each source organ was distinctly visible for ROI definition at at least one time point. For the lungs, drawing of ROIs was facilitated by using transmission images, which delineated the lung boundaries well. Lung ROIs were conservatively drawn to avoid spillover activity from the heart and liver. ROIs drawn at the time of maximum organ activity were applied to time points of lesser organ activity. The specific measurement time assigned to each organ was the estimated midpoint of the time that the organ was in the scanner field of view during each of the sequential whole-body scans.

ROI kinetic data for all source organs were fit in a least-squares sense with exponential functions of the type:

$$A(t) = \sum_i \alpha_i e^{-\lambda_i t},$$

where A(t) is the model activity as a function of time. Nonlinear regression was used to vary the parameters α_i and λ_i until a fit satisfactory for dosimetry was achieved. Residence times were determined by integration of these empirically determined functions from time zero to infinity (including physical decay). All activity in the heart ROI was conservatively assumed to be in the heart wall. All unaccounted-for activity was assumed to be indefinitely retained in remainder tissues, the S-value of which was determined according to the standard MIRD approach.

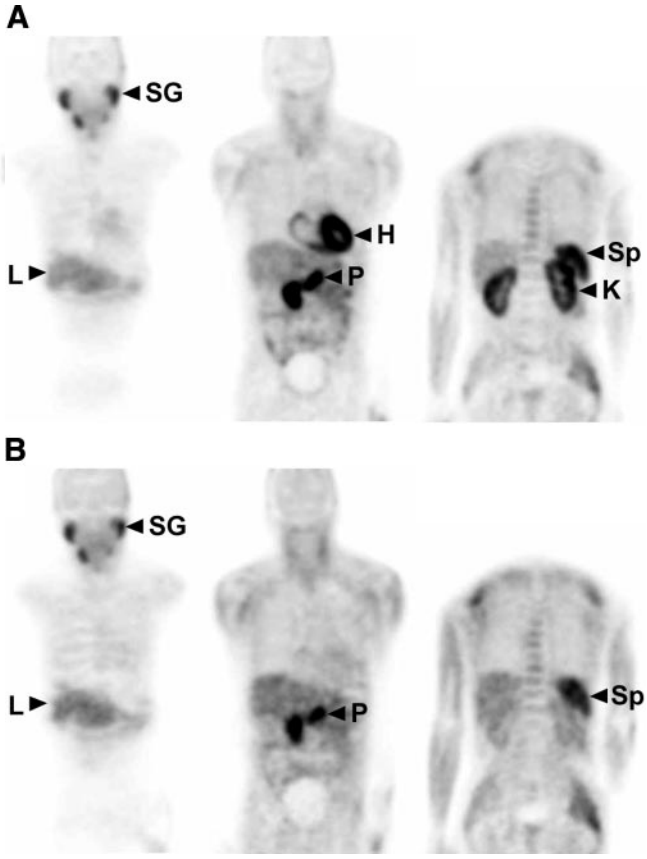

FIGURE 2. Representative coronal planes of whole-body ^{11}C-acetate PET images at 2 min (A) and 28 min (B) after injection. Early scan shows intense tracer uptake in salivary glands, heart, pancreas, kidneys, and spleen. Late scan shows tracer clearance from heart and kidneys and tracer retention in salivary glands, pancreas, liver, and spleen. L = liver; H = heart; K = kidney; P = pancreas; SG = salivary glands; Sp = spleen.

TABLE 1
Residence Time (Hours) of ^{11}C-Acetate for Measured Source Organs

Organ	Subject Number						Mean	SD
	1	2	3	4	5	6		
Stomach wall	1.7E-03	2.0E-03	8.5E-04	2.6E-03	8.6E-04	2.1E-03	1.7E-03	7.1E-04
Bowel	3.5E-02	4.0E-02	2.9E-02	4.7E-02	2.1E-02	3.6E-02	3.5E-02	9.0E-03
Heart wall	5.4E-03	6.4E-03	5.3E-03	7.0E-03	7.2E-03	5.8E-03	6.2E-03	8.1E-04
Kidneys	9.2E-03	1.0E-02	5.9E-03	6.3E-03	7.4E-03	1.2E-02	8.5E-03	2.4E-03
Liver	4.2E-02	4.2E-02	2.0E-02	3.4E-02	1.4E-02	2.2E-02	2.9E-02	1.2E-02
Lungs	1.8E-02	1.7E-02	9.1E-03	8.2E-03	1.4E-02	1.3E-02	1.3E-02	4.0E-03
Pancreas	3.6E-03	6.3E-03	3.8E-03	6.0E-03	8.0E-03	6.5E-03	5.7E-03	1.7E-03
Salivary	3.7E-04	6.3E-04	7.5E-04	4.2E-04	8.5E-04	5.2E-04	5.9E-04	1.9E-04
Spleen	2.4E-03	6.3E-03	3.4E-03	5.5E-03	3.4E-03	1.0E-02	5.2E-03	2.8E-03
Red marrow	2.6E-02	3.5E-02	2.5E-02	5.0E-02	4.2E-02	3.4E-02	3.5E-02	9.5E-03
Remainder	3.5E-01	3.2E-01	3.9E-01	3.2E-01	3.7E-01	3.5E-01	3.5E-01	2.8E-02

Absorbed Dose Estimates

Absorbed dose was estimated using the absorbed fractions for the reference adult male phantom developed by Cristy and Eckerman (*11*) and using MIRDOSE3.1 (*12*). For the salivary glands, the S-value was conservatively assumed to be the same as for a single soft-tissue sphere, with mass equal to that of the combined salivary glands. Effective dose equivalent and effective dose were determined using the methodology described in International Commission on Radiological Protection (ICRP) publications 30 (*13*) and 60 (*14*), respectively.

RESULTS

Visual inspection of PET images demonstrated rapid accumulation of activity in the heart, kidneys, liver, pancreas, spleen, stomach, bowel, and bone marrow. The time–activity curves for the mean decay-corrected percentage injected dose for each organ are shown in Figure 3. The residence times for each measured source organ are shown in Table 1. The mean dose estimates for ^{11}C-acetate are shown in Table 2 and are compared with the reported ORISE dose estimates.

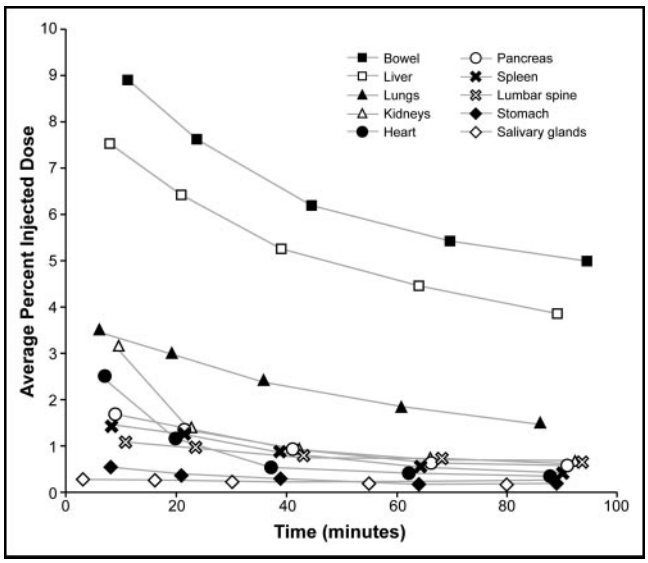

FIGURE 3. Time–activity curves of the mean decay-corrected percentage injected dose in all measured source organs.

As expected, for most organs that were not considered in the ORISE model and that showed significant measurable

TABLE 2
Absorbed Dose Estimates for ^{11}C-Acetate (mGy/MBq)*

Target organ	Mean	ORISE values†
Adrenals	3.4E-03 (2)	3.2E-03
Brain	2.1E-03 (6)	1.8E-03
Breasts	2.2E-03 (4)	3.0E-03
Gallbladder wall	3.7E-03 (5)	2.7E-03
Lower large intestine wall	1.0E-02 (20)	2.2E-03
Small intestine	1.0E-02 (20)	2.3E-03
Stomach	3.3E-03 (12)	3.0E-03
Upper large intestine wall	1.1E-02 (21)	2.3E-03
Heart wall	6.6E-03 (10)	9.7E-02
Kidneys	9.2E-03 (23)	2.4E-03
Liver	6.0E-03 (33)	3.0E-03
Lungs	4.6E-03 (22)	1.8E-02
Muscle	2.5E-03 (4)	2.3E-03
Ovaries	3.6E-03 (3)	2.2E-03
Pancreas	1.7E-02 (26)	3.5E-03
Red marrow	5.7E-03 (17)	2.7E-03
Bone surfaces	4.4E-03 (12)	2.3E-03
Salivary glands†‡	3.4E-03 (32)	NE
Skin	2.0E-03 (5)	1.8E-03
Spleen	9.2E-03 (45)	2.7E-03
Testes	2.3E-03 (6)	1.8E-03
Thymus	2.6E-03 (5)	4.6E-03
Thyroid	2.4E-03 (6)	2.2E-03
Urinary bladder wall	2.8E-03 (4)	2.1E-03
Uterus	3.3E-03 (2)	2.3E-03
Total body	2.9E-03 (0)	3.0E-03
EDE (mSv/MBq)	6.2E-03 (11)	1.0E-02
ED (mSv/MBq)	4.9E-03 (8)	4.5E-03

*To obtain the dose estimates in rad/mCi, multiply by 3.7.
†ORISE Dose Estimates Table, ^{11}C-acetate, 1995.
‡Self-dose only.
NE = not estimated; EDE = effective dose equivalent; ED = effective dose.
Data in parentheses are percentage SD.

activity, the absorbed doses were significantly higher than those listed in the ORISE table. The organs that received the highest absorbed doses were the pancreas (0.017 mGy/MBq), bowel (0.011 mGy/MBq), kidneys (0.0092 mGy/MBq), spleen (0.0092 mGy/MBq), heart (0.0066 mGy/MBq), and liver (0.006 mGy/MBq). There was no measurable urinary excretion of tracer, nor was there any measurable tracer uptake in the brain. The effective dose was 0.0049 mSv/MBq. The effective dose equivalent was 0.0062 mSv/MBq.

DISCUSSION

The measured radiation-absorbed doses in the critical organs and in most secondary organs differ markedly from previously determined ORISE estimates. Because the dosimetry methodologies used by us and by ORISE were essentially identical, the difference between the dose estimates obtained here and the dose estimates obtained by ORISE is almost certainly due to the difference in the biodistribution data used to create the kinetic models. In the ORISE estimates, the data were limited to measurements of activity in the blood and in expired air from the lungs, and conservative assumptions regarding the unaccounted-for activity had to be made. Because the kinetic data that were used here were more complete, representing all major source organs, more accurate dosimetry estimates were possible.

The current dose estimates indicate that the critical organ is the pancreas, with an average absorbed dose of 0.017 mGy/MBq. This is consistent with previous work demonstrating high ^{11}C-acetate tracer uptake and retention in the pancreas relative to other organs (*15*). The high ^{11}C tracer concentration within the pancreas is believed to be due to a high rate of lipid synthesis within pancreatic acinar cells. The lack of measurable renal excretion of tracer supports previous clinical studies demonstrating minimal urinary excretion and the potential advantage of ^{11}C-acetate PET for evaluating pelvic malignancies (*16*,*17*).

CONCLUSION

Under the previous ORISE estimates, the dose-limiting organ was the heart, with a dose estimate that imposed a maximum injected dose of 525 MBq to satisfy the federal Radioactive Drug Research Committee limit of 50 mSv (5 rem) to an individual organ (*18*). Using the dose estimates reported here, the dose-limiting organ is the pancreas and the maximum injected dose of ^{11}C-acetate PET under Radioactive Drug Research Committee guidelines can be raised up to 5-fold over the limit imposed by the ORISE estimates. The ability to administer a higher injected dose would be beneficial for lengthy whole-body acquisitions, which typically require imaging times that exceed the physical half-life of the short-lived radioisotope ^{11}C. Administering more activity will improve counting statistics and, it is hoped, result in better image quality and tumor detection with whole-body ^{11}C-acetate PET.

ACKNOWLEDGMENTS

This work was supported by grants from the Department of Energy (contract DE-FC03-87-ER60615) and the California Cancer Research Program, grant 6485 from the California Department of Health Services, and the CaP CURE Foundation.

REFERENCES

1. Shreve PD. Carbon-11 acetate PET imaging of prostate cancer [abstract]. *J Nucl Med.* 1999;40(suppl):60P.
2. *Dose Estimate Table for C-11 Acetate.* Oak Ridge, TN: Radiation Internal Dose Information Center, Oak Ridge Institute for Science and Education; 1995.
3. Oyama N, Akino H, Kanamaru H, et al. ^{11}C-Acetate PET imaging of prostate cancer. *J Nucl Med.* 2002;43:181–186.
4. Muranoto S, Yamamoto K, Ohyama N, et al. Positive imaging of prostate cancer with carbon-11 acetate and PET [abstract]. *J Nucl Med.* 1999;40(suppl):60P.
5. Shields AF, Graham MM, Kozawa SM, et al. Contribution of labeled carbon dioxide to PET imaging of carbon-11-labeled compounds. *J Nucl Med.* 1992;33:581–584.
6. Dahlbom M, Hoffman EJ, Hoh CK, et al. Whole-body positron emission tomography: part I. Methods and performance characteristics. *J Nucl Med.* 1992;33:1191–1199.
7. Adam LE, Zaers J, Ostertag H, Trojan H, Bellemann M, Brix G. Performance evaluation of the whole-body PET scanner ECAT EXACT HR+ following the IEC standard. *IEEE Trans Nucl Sci.* 1997;44:1172–1179.
8. Meikle SR, Hutton BF, Bailey DL, Hooper PK, Fulham MJ. Accelerated EM reconstruction in total-body PET: potential for improving tumour detectability. *Phys Med Biol.* 1994;39:1689–1704.
9. Qi J, Leahy RM. A theoretical study of the contrast recovery and variance of MAP reconstructions from PET data. *IEEE Trans Med Imaging.* 1999;18:293–305.
10. Oberdorfer F, Theobald A, Prenant C. Simple production of [1-carbon-11]acetate. *J Nucl Med.* 1996;37:341–342.
11. Cristy M, Eckerman KF. *Specific Absorbed Fractions of Energy at Various Ages from Internal Photon Sources.* Oak Ridge, TN: Oak Ridge National Laboratory; 1987.
12. Stabin MG. MIRDOSE: personal computer software for internal dose assessment in nuclear medicine. *J Nucl Med.* 1996;37:538–546.
13. ICRP-30: limits for intakes of radionuclides by workers. *Ann ICRP.* 1981;6:1–124.
14. ICRP-60: 1990 recommendations of the International Commission on Radiological Protection. *Ann ICRP.* 1991;21:1–201.
15. Shreve PD, Gross MD. Imaging of the pancreas and related diseases with PET carbon-11-acetate. *J Nucl Med.* 1997;38:1305–1310.
16. Oyama N, Miller TR, Dehdashti F, et al. ^{11}C-Acetate PET imaging of prostate cancer: detection of recurrent disease at PSA relapse. *J Nucl Med.* 2003;44:549–555.
17. Oyama N, Miller TR, Dehdashti F, et al. Carbon-11-acetate PET imaging of recurrent prostate cancer. *J Urol.* 2002;167:173–174.
18. *Code of Federal Regulations 21CFR 361.1.* Washington, DC: U.S. Department of Health and Human Services; 1984.